

# LaFiTe: A Generative Latent Field for 3D Native Texturing

Chia-Hao Chen<sup>1</sup> Zi-Xin Zou<sup>2</sup> Yan-Pei Cao<sup>2</sup>  
 Ze Yuan<sup>3</sup> Guan Luo<sup>1</sup> Xiaojuan Qi<sup>3</sup> Ding Liang<sup>2</sup> Song-Hai Zhang<sup>1†</sup> Yuan-Chen Guo<sup>2†</sup>

<sup>1</sup>Tsinghua University <sup>2</sup>VAST <sup>3</sup>The University of Hong Kong



Figure 1. A gallery of diverse 3D assets textured by our 3D-native framework, LaFiTe, demonstrating **high-fidelity, seamless textures across a wide range of visual styles**.

## Abstract

Generating high-fidelity, seamless textures directly on 3D surfaces, what we term 3D-native texturing, remains a fundamental open challenge, with the potential to overcome long-standing limitations of UV-based and multi-view projection methods. However, existing native approaches are constrained by the absence of a powerful and versatile latent representation, which severely limits the fidelity and generality of their generated textures. We identify this representation gap as the principal barrier to further progress. We introduce LaFiTe, a framework that addresses this chal-

lenge by learning to generate textures as a 3D generative sparse latent color field. At its core, LaFiTe employs a variational autoencoder (VAE) to encode complex surface appearance into a sparse, structured latent space, which is subsequently decoded into a continuous color field. This representation achieves unprecedented fidelity, exceeding state-of-the-art methods by **>10 dB PSNR** in reconstruction, by effectively disentangling texture appearance from mesh topology and UV parameterization. Building upon this strong representation, a conditional rectified-flow model synthesizes high-quality, coherent textures across diverse styles and geometries. Extensive experiments demonstrate that LaFiTe not only sets a new benchmark for 3D-

† Corresponding authors

native texturing but also enables flexible downstream applications such as material synthesis and texture super-resolution, paving the way for the next generation of 3D content creation workflows.

## 1. Introduction

The automated generation of high-quality 3D content has become a cornerstone of modern computer graphics and vision. While significant strides have been made in generating complex 3D geometry [68, 79], the creation of detailed, seamless, and coherent textures remains a major bottleneck. Textures often contribute more to the visual richness and realism of an asset than the geometry itself. As such, developing powerful generative models for texturing is a critical and defining challenge for the next generation of AI-driven content creation.

Current approaches for texture generation predominantly fall into two categories, both of which are inherited from 2D-centric paradigms and suffer from fundamental limitations. The most common approach involves generating multiple 2D images of an object from different viewpoints and then projecting them back onto the mesh surface [10, 25, 40, 43, 51]. This “multi-view projection” strategy is inherently flawed - it struggles to reconcile inconsistent predictions caused by cross-view misalignment, occlusions, and view-dependent lighting, inevitably leading to conspicuous seams and artifacts that require complex post-processing to fix. An alternative approach is to generate textures directly in a 2D UV-unwrapped space [75]. However, this method trades one set of problems for another. It becomes critically dependent on a mesh’s UV parameterization, which is non-unique and often introduces severe distortions, leading to textures that are warped or contain seams along UV island boundaries. These approaches are symptomatic treatments, not a cure for the underlying challenge of creating truly 3D-native appearance.

We argue that the only way to guarantee spatial coherence and seamlessness is to generate textures *directly in 3D space*. This native approach sidesteps the inherent contradictions of 2D-based methods. If this path is so clearly superior, why has it not yet dominated? The central roadblock, and the primary focus of this work, has been the lack of a suitable **3D texture representation**. An ideal representation for generative modeling must satisfy three criteria: it must be **expressive** enough to capture high-frequency details; it must be **decoupled** from the mesh’s specific topology and UV coordinates; and it must be **compact and structured** enough to be learned effectively by a generative model.

To address this critical representation gap, we introduce **LaFiTe**, a framework built on the central insight that a powerful generative model of 3D textures must rely on a pow-

erful representation. We propose to model 3D texture as a **sparse latent color field**, and design a novel variational autoencoder (VAE) to learn this color field from data. Our VAE encodes the appearance of a 3D asset, represented as a dense colored point cloud, into a sparse, structured latent feature. This representation is powerful because it is **local and continuous**; it concentrates modeling capacity near the object’s surface and can be queried at any point in space to reconstruct fine-grained details. This fundamentally disentangles texture from the discrete, and often problematic, mesh connectivity and UV coordinates.

Furthermore, LaFiTe introduces a second key insight into the geometry conditioning of the generative process. We found that the geometry of the mesh is implicitly but accurately captured by our VAE encoder. By encoding an untextured (“monochrome”) version of the mesh, we can extract a geometry latent that provides a complete, occlusion-free 3D shape guidance. This elegant maneuver allows us to condition our generative model on a perfect 3D geometric signal that is inherently aligned with the texture representation, without the need for a separate geometry encoder. This synergistic design of representation and conditioning is the key to LaFiTe’s ability to synthesize textures with state-of-the-art quality and coherence.

Our main contributions are summarized as follows.

- **A High-Fidelity Latent Color Field Representation:** We are the first to propose and learn a latent color field for native texturing, achieving state-of-the-art reconstruction fidelity ( $>10$  dB PSNR improvement over prior work) while being fully decoupled from the mesh topology.
- **A Unified Texture Generation Framework:** We achieve 3D texturing by generating the latent color field using flow matching, and introduce a highly effective method for geometry conditioning by reusing our texture encoder to encode a monochrome point cloud.
- **State-of-the-Art Native Texturing:** LaFiTe significantly outperforms all existing native and projection-based methods, delivering seamless, detailed, and coherent textures across a diverse range of complex 3D assets.

## 2. Related Work

**3D Representations and Generative Models.** The field of 3D content generation has rapidly evolved, driven by advances in both underlying 3D representations and the neural models that create them. Research has explored a wide range of representations, from implicit fields like SDFs [13, 53] and UDFs [21, 53] to explicit structures like meshes [12, 49, 61], point clouds, and 3D Gaussians [33]. The generative models and methods themselves have progressed from score-based distillation [23, 39, 55, 65, 66, 74] on differentiable representations to powerful 3D-native models. A key component in many modern systems is the intermediate neural representation, such as tri-

planes [9, 28, 36, 80, 85], sparse latents [24, 67, 68], or VecSets [37, 64, 79, 81], which encode 3D information for the generative model. While this body of work provides the foundation, it has largely focused on geometry; our work tackles the distinct challenge of a generative representation for 3D texture.

**Multi-View Image Generation.** A recent common paradigm for 3D texturing is to synthesize multiple 2D views and project them onto a mesh. Initial works, enabled by powerful 2D diffusion models, faced a trade-off between slow, per-object optimization [22] and progressive generation [8, 10, 58] that risked view misalignment. Subsequent research has therefore focused on improving multi-view consistency [14, 19, 43, 45], either by synchronizing the denoising process across views or by jointly generating all views [6, 25, 31, 40, 71, 76, 81]. Orthogonal to consistency, a major thrust has been generating physically-based rendering (PBR) materials [7, 11, 18, 25, 29, 30, 48, 62, 72, 82, 84] to support realistic relighting [27, 34, 78]. While increasingly sophisticated, these methods all grapple with the fundamental ill-posedness of reconciling multiple 2D images into a single, coherent 3D surface, a problem our native approach sidesteps entirely.

**Native Texture Generation.** To circumvent the inherent issues of 2D projection, native approaches generate texture directly in the object’s own space. Some methods operate in a 2D UV-unwrapped space [73, 75, 76], but this makes them dependent on a non-unique and often distorted parameterization. A more robust direction, and the one we pursue, is to represent textures natively in 3D. Prior works have explored this by learning on mesh surfaces [60], 3D texture fields [32, 40, 51, 68, 69], and generating colored point clouds or 3DGS [41, 70, 73] to define spatial texture. However, these pioneering native works have been limited by their chosen representations, which can struggle to capture high-frequency detail within a compact latent space suitable for high-fidelity generative modeling.

### 3. Method

We introduce LaFiTe, a generative framework for seamless, high-fidelity native texturing on arbitrary mesh topologies. At its core is a novel latent representation of 3D texture, which we detail along with its encode-decode architecture (Sec. 3.1). We then describe our conditional generation model (Sec. 3.2), various downstream applications (Sec. 3.3), and our data curation pipeline (Sec. 4).

#### 3.1. The LaFiTe Representation: A VAE for Sparse Latent Color Field

Unlike dense representations such as triplanes [9, 59] or dense grids [47], we adopt a more efficient sparse structure that has been widely used in recent advanced models [24, 38, 68]. Specifically, we discretize 3D space into a voxel grid, storing information only in active voxels near the object’s surface. Within each active voxel, a continuous implicit function defines the local color field. This hybrid approach efficiently concentrates modeling capacity and memory, handles arbitrary topology, and enables the querying of continuous, high-frequency details. To learn this representation, we design a variational autoencoder (VAE) that maps a densely sampled colored points to a compact, sparse-structured latent space, from which the continuous color field is subsequently decoded.

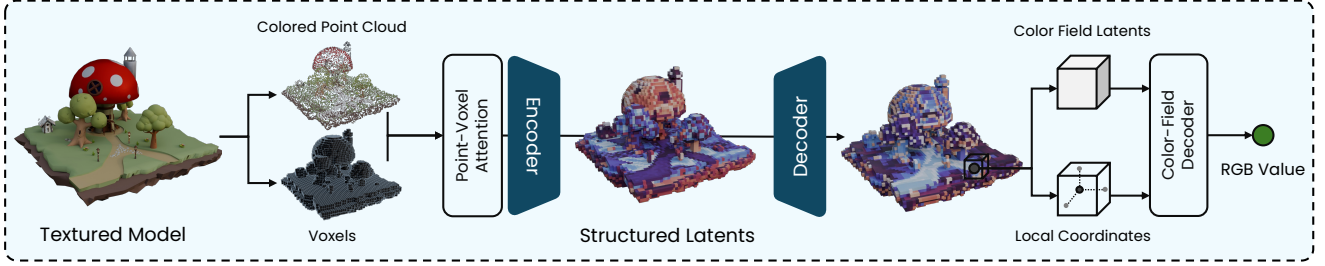
**Texture Encoding.** Recent 3D generative models [68] typically achieve this by projecting pre-trained 2D features (e.g., DINO [52, 63]) from multiple camera views onto the on-surface sparse voxels. While effective, this strategy exhibits three fundamental limitations: (1) The projection process is view-dependent, causing inconsistencies or ambiguity in occluded regions; (2) Pretrained 2D features have limited resolution, restricting high-frequency surface details; (3) Features are tied to the 2D foundation knowledge, which may not optimally represent fine-grained 3D surface attributes such as PBR materials.

In contrast, we propose constructing a representation that directly and unbiasedly captures the high-fidelity texture of a 3D asset by using a colored point cloud  $\mathcal{P} = \{x_i = (p_i, n_i, c_i)\}$  densely sampled from the textured mesh. Specifically, we uniformly sample points  $p_i$  together with their corresponding normals  $n_i$  and raw colors  $c_i$ , which serve as the input to the texture encoder. This provides the encoder with native, unoccluded, and view-independent surface information, minimizing information loss and forming a more accurate ground truth for representation learning.

Given this point cloud, we adopt an encoder architecture similar to SparseFlex [24], but replacing the PointNet [56] with a specialized point-voxel attention mechanism for robustly fusing point features within each voxel. This encoder compresses the detailed, high-frequency texture information into sparse, structured latent features  $\mathcal{Z} = \{z_k\}$ , where  $k$  indexes the set of  $L$  on-surface voxels. The point-voxel attention mechanism comprises an intra-voxel self-attention module and a point-voxel cross-attention module.

The intra-voxel self-attention module processes all points within each voxel, allowing them to interact and aggregate local geometric and appearance features into a set

## Color-Geometry Encoding & Color Field Decoding



## Geometry-Conditioned Texture Generation

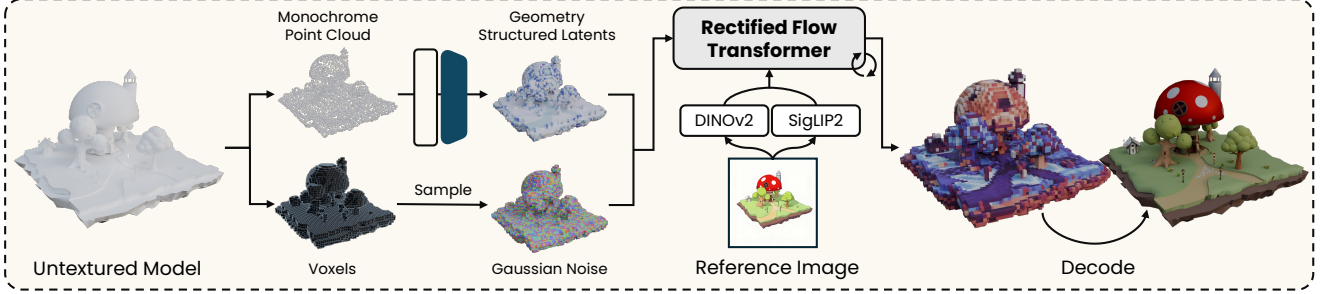


Figure 2. **The LaFiTe Pipeline.** (Top) A VAE autoencoder learns a sparse latent color field representation by encoding a colored point cloud sampled from the mesh surface. (Bottom) For generation, the VAE encoder first extracts a geometry latent from a monochrome point cloud. This geometry latent then conditions a rectified flow model to synthesize a texture latent, which is decoded to the 3D texture.

of point-wise features  $\tilde{x}$ :

$$\tilde{x}_i = \sum_{j=1}^n \text{softmax}\left(\frac{Q_{x_i} K_{x_j}^T}{\sqrt{d}}\right) \cdot V_{x_j}, \quad (1)$$

where  $x_j$  denotes the initial point features within the same voxel as  $x_i$ .

The point-voxel cross-attention module then consolidates these detailed point-wise features into voxel-wise features  $\tilde{v}_k$ , representing the encoded texture information for each voxel. This is achieved by attending from a shared learnable voxel feature  $v_k$  to all point-wise features within the voxel:

$$\tilde{v}_k = \sum_{i=1}^n \text{softmax}\left(\frac{Q_{v_k} K_{\tilde{x}_i}^T}{\sqrt{d}}\right) \cdot V_{\tilde{x}_i}. \quad (2)$$

This design ensures robust capturing the local surface appearance than the average pooling in PointNet. The resulting set of voxel embeddings  $\{\tilde{v}_k\}$  is then passed through a standard sparse-voxel-based VAE encoder [24, 68] with shifted window attention to produce the final latent codes  $\{z_k\}$ . The overall texture encoding process is as follows:

$$\mathcal{E} : \{\{x_j\}_{j=1}^{N_i}\}_{i=1}^L \rightarrow \{z_k\}_{k=1}^L. \quad (3)$$

**Implicit Geometry Encoding.** A crucial property of our encoder is that, besides encoding texture, it naturally captures high-fidelity geometry from the point cloud positions

at no extra cost. We exploit this by introducing a *pure geometry latent*: passing a monochrome point cloud – setting all input colors  $c_i$  to a canonical value like white  $(1, 1, 1)$  – we effectively factor out texture information. The resulting geometry latent  $z_{\text{geo}}$  represents only the object’s shape. This elegant approach provides an occlusion-free 3D geometric prior for our generative model without a separate geometry network, while ensuring perfect alignment between the shape and texture conditions during synthesis.

**Texture Decoding and Supervision.** The decoder’s role is to reconstruct the continuous color field  $\mathcal{C}(p)$  from the sparse, structured latent representation  $\{z_k\}$ . For any 3D query point  $p$  within a voxel  $k$ , a latent decoder  $\mathcal{D}_S$  first maps the corresponding latent  $z_k$  to a higher-resolution local feature grid  $f_k$ . This local feature grid forms a sparse local color field, from which the color decoder  $\mathcal{D}_F$  takes features interpolated using the local coordinates of  $p$  and outputs the final RGB color  $c$  through a shallow MLP. The overall VAE decoder is as follows:

$$\mathcal{D} : \{z_k\}_{k=1}^L \times p_j \rightarrow c_j. \quad (4)$$

We train the VAE end-to-end using a reconstruction loss combined with a KL divergence regularization term. The reconstruction loss is a simple L1 loss on the color values of sampled points, which we find effectively promotes sharp details. To encourage the model to learn a robust representation of high-frequency textures, we augment input colors with minor Gaussian noise during training. The overall

VAE objective is given by:

$$\mathcal{L} = \mathbb{E}_{x_i \sim \mathcal{M}}[|\mathcal{D}(\mathcal{E}(\{\hat{x}_i\}), p_j) - \hat{c}_j|] + \mathcal{L}_{\text{KL}}. \quad (5)$$

where  $\hat{x}_i = (p_i, n_i, \hat{c}_i)$ ,  $\hat{c}_i = c_i + \epsilon$  is the augmented color. Importantly, we do not rely on rendering-based losses (like LPIPS or SSIM), which can introduce blurriness and bias. Instead, supervision is performed directly in the 3D space, ensuring the learned representation faithfully models the underlying surface texture.

### 3.2. Conditional Texture Synthesis via Rectified Flow

Having established a powerful latent representation for 3D textures, we now detail the generative process for synthesizing novel textures within this space. We employ a conditional rectified flow [35, 42] model, which learns to generate texture latents  $z$  conditioned on the geometry of the input mesh and a reference image.

**Geometry-Conditioned Albedo Generation.** The cornerstone of our synthesis pipeline is the generation of a base color (albedo) texture. The quality of this generation depends critically on the fidelity of the geometric conditioning. Unlike methods that rely on 2D geometric projections (e.g., position or normal maps), which suffer from occlusions and cross-view inconsistencies, our approach conditions directly on the complete and unambiguous 3D shape.

Specifically, we use the pure geometry latent  $z_{\text{geo}}$ , derived as described in Sec. 3.1, as the primary condition. This provides the generative model with a detailed, occlusion-free 3D geometry prior that is perfectly aligned with the target latent space. The model is trained using the conditional flow matching objective:

$$\mathcal{L}_{\text{albedo}} = \mathbb{E}\|v(x_t; t, z_{\text{geo}}) - (\epsilon - x_0)\|, \quad (6)$$

where  $c_{\text{geo}}$  is the geometry condition represented by  $\mathcal{E}(\{p_i, n_i, \mathbf{1}\})$ , and  $x_t$  is the noisy latent in timestep  $t$ ,  $x_t = (1 - t)x_0 + t\epsilon$ . We adopt a progressive training strategy: The model is first trained on latents at  $64^3$  resolution, and then fine-tuned on  $128^3$  resolution latents, which are encoded from a denser point cloud sampling.

**Disentangled PBR Material Generation.** Our framework naturally extends to generating physically-based rendering (PBR) materials by learning to synthesize roughness and metallic maps. A key insight is that these material properties are often physically correlated with the underlying albedo; therefore, conditioning solely on geometry is sub-optimal. We leverage this insight to create a disentangled, hierarchical generation process. Instead of conditioning on the pure geometry latent, we fine-tune our albedo generation model to synthesize roughness-metallic latents conditioned on the *albedo latent*  $z_{\text{albedo}}$  (either from the user input or a previously generated sample). This hierarchical

approach – i.e., geometry  $\rightarrow$  albedo, then albedo  $\rightarrow$  PBR – more faithfully models the physical dependencies and leads to more plausible and detailed material generation.

For implementation, we reuse the pretrained color texture VAE by simply replacing its three color channels with roughness, metallic, and an additional zero-padding channel. We then train the model with a similar flow matching objective  $\mathcal{L}_{\text{RM}}$ , additionally conditioned on the albedo latent. This design enables fully disentangled control over the final material appearance.

### 3.3. Interfacing and Interaction with LaFiTe

A key advantage of our sparse latent color field is its versatility. Beyond synthesis, the learned representation serves as a powerful asset that seamlessly integrates into existing 3D workflows and manipulated for fine-grained artistic control.

**Texture Baking for Standard Pipelines.** To integrate with standard rendering engines, our continuous 3D color field  $\mathcal{C}(p)$  is “baked” [20, 50] into a 2D UV texture map. Unlike multi-view projection methods [25, 43] that struggle to resolve inconsistent predictions, our native 3D representation makes this process straightforward and robust. Baking simply involves querying our learned function  $\mathcal{C}(p)$  for each corresponding 3D point on the UV map. To produce anti-aliased textures, we supersample by averaging the colors of multiple random points within each pixel’s footprint. Because our underlying field is inherently seamless, this process yields clean texture maps free of the seams and artifacts that plague projection-based methods.

**Local Refinement.** Our framework naturally supports local texture alteration. Adapting techniques like RePaint [46], a user-defined target mesh region can be mapped to its corresponding latent voxels, which are then regenerated while keeping surrounding regions unchanged. This 3D-native local regeneration process is inherently more coherent than 2D UV repainting, as it respects the underlying geometry to ensure seamless transitions at local boundaries. This process can be utilized to achieve local texture refinement in areas where higher resolution textures are demanded. See Sec.5.4 for more details.

## 4. Principled Data Curation

Large-scale 3D datasets [15, 16] are notoriously uncurated and contain ambiguous signals. We therefore employ a principled data curation pipeline to normalize assets and ensure that our model learns from clean data.

**Resolving Material Ambiguity.** Public datasets contain assets with non-standard materials, such as emissive channels, that create ambiguous training signals. Our pipeline canonicalizes these materials: (1) for fully emissive surfaces, we use the emission map as the base color, as environmental lighting is irrelevant; (2) for partially emissive

Table 1. **Quantitative comparison for conditional texture generation.** We evaluate LaFiTe against leading text- and image-conditioned texture generation methods. LaFiTe achieves superior or competitive performance across nearly all metrics, demonstrating its state-of-the-art generation quality. *Lower is better for all metrics.*

Method	Condition	Unshaded					Shaded				
		FID↓	FD <sub>CLIP</sub> ↓	FD <sub>DINO</sub> ↓	KD <sub>CLIP</sub> ↓	KD <sub>DINO</sub> ↓	FID↓	FD <sub>CLIP</sub> ↓	FD <sub>DINO</sub> ↓	KD <sub>CLIP</sub> ↓	KD <sub>DINO</sub> ↓
MVPaint [14]	Text	158.28	96.86	140.70	0.153	0.184	135.94	84.53	118.85	0.117	0.120
MaterialAnything [30]	Text	165.50	96.89	115.72	0.166	0.129	126.00	74.76	108.78	0.090	0.125
SyncMVD [43]	Text	126.20	76.25	88.17	0.072	0.060	119.38	66.87	80.99	0.058	0.047
TEXGen [75]	Text+Image	136.58	86.18	106.66	0.114	0.094	130.29	77.62	97.25	0.088	0.080
SeqTex [76]	Text+Image	119.31	61.58	76.14	0.041	0.033	116.72	62.20	74.44	0.051	0.032
Paint3D [77]	Text/Image	124.73	69.72	86.47	0.084	0.059	116.61	61.70	80.28	0.063	0.050
MaterialMVP [25]	Image	113.20	54.79	67.67	0.048	0.029	101.66	48.71	66.83	0.035	0.032
UniTEX [40]	Image	106.45	51.08	69.74	0.036	0.034	105.75	51.62	69.65	0.038	0.034
Ours	Image	107.46	53.49	67.16	0.037	0.032	101.91	46.28	64.19	0.026	0.027

ones, we composite the base and emission colors with a tone mapping operator to prevent value clipping and preserve the asset’s visual intent. This ensures the final color fed to our VAE remains within a valid, consistent range, preserving the visual intent of the original asset.

**Resolving Geometric Ambiguity.** Real-world 3D assets also contain non-standard geometry, e.g., stylized “outline” shells, designed for specific rendering effects. These components can corrupt the surface sampling process, as points sampled on them may be incorrectly associated with voxels of the primary object, leading to a noisy latent representation. Our curation pipeline automatically identifies and discards such geometry using heuristics based on rendering properties (e.g., backface culling, inverted normals), ensuring the VAE learns only from the intended visible surface.

**High-Fidelity Surface Sampling.** The fidelity of our latent representation depends on the density and quality of the input point cloud. To capture high-frequency textures and ensure full mesh coverage – including small triangles and UV-distorted regions – we employ a denser surface sampling strategy (2 million points uniformly sampled from each 3D model) to train the VAE. For diffusion model training, we cache latents from an even denser cloud of 5 million points to provide the highest-quality latent encoding. This dense sampling creates a lossless ground truth, enabling our model to generate more fine-grained textures.

## 5. Experiments

We validate LaFiTe through comprehensive experiments. We benchmark our core VAE representation (Sec. 5.2), evaluate the full generative pipeline against state-of-the-art methods (Sec. 5.3), and showcase downstream applications (Sec. 5.4).

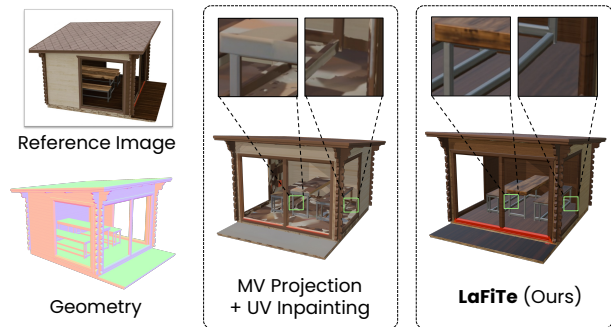


Figure 3. **Robustness to self-occlusion.** LaFiTe’s 3D-native formulation generates complete and coherent textures even in highly occluded regions where projection methods fail.

### 5.1. Implementation Details

We train LaFiTe on a large-scale dataset of 1M textured 3D assets collected from Objaverse [16], Objaverse-XL [15], and TexVerse [83]. Our VAE is trained for 600K steps using 16 NVIDIA A800 GPUs with a batch size of 256. The rectified flow model for albedo generation is trained for 500K steps on 32 NVIDIA A800 GPUs. We employ a progressive curriculum, first training on latents from a  $64^3$  voxel grid, then fine-tuning on higher-fidelity  $128^3$  latents. The PBR generator is then fine-tuned from the final albedo model by switching to a PBR material target. All models are trained using the AdamW optimizer [44] with a constant learning rate of  $1e - 4$ .

### 5.2. Analysis of the LaFiTe Representation

We first validate the central claim of our work by evaluating the reconstruction fidelity of our VAE representation.

**Setup.** We compare our VAE against TRELIS [68], a state-of-the-art model that represents texture by projecting pre-trained 2D DINO [52] features onto the volume as input. For a fair comparison, both models are tasked with reconstructing the original ground-truth texture from their

Table 2. **VAE Reconstruction Fidelity.** Our VAE, which uses a direct point cloud input, achieves significantly higher fidelity than TRELIS, which uses projected image features. “\*” denotes the result is derived from the 64 resolution model without training on higher resolutions.

Method	PSNR $\uparrow$	SSIM $\uparrow$	LPIPS $\downarrow$
TRELIS-GS64	21.37	0.833	0.116
TRELIS-RF64	21.83	0.864	0.108
TRELIS-GS128*	19.28	0.787	0.195
TRELIS-RF128*	23.07	0.880	0.127
Ours-64	33.57	0.960	0.053
Ours-128*	34.48	0.965	0.041
Ours-128	<b>34.62</b>	<b>0.967</b>	<b>0.039</b>

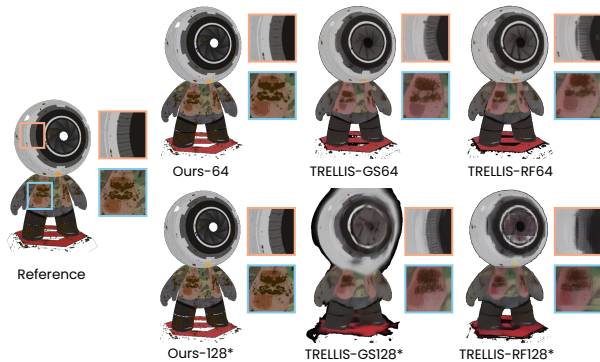


Figure 4. **Visual comparison of VAE reconstruction quality.** Our method reconstructs sharper, more detailed textures, avoiding the blurs and artifacts of the TRELIS baseline.

learned latent representations. We evaluate performance using standard image-space metrics (PSNR, SSIM, LPIPS) computed across multiple rendered views.

**Results.** As demonstrated in Tab. 2 and Fig. 4, LaFiTe achieves dramatically higher reconstruction quality across all metrics and resolutions, culminating in a *PSNR improvement of over 10 dB* at the 128<sup>3</sup> resolution. This result provides clear evidence for our hypothesis: directly encoding a pristine 3D colored point cloud captures high-frequency surface information far more faithfully than projecting and aggregating 2D features, which inherently suffer from resolution limits, view inconsistencies, and projection ambiguities.

**Scalability with Sampling Density.** We further analyze the scalability of our representation with respect to the density of the input point cloud. As shown in Tab. 3, reconstruction quality improves consistently with denser sampling. This confirms our model’s capacity to leverage richer input data and validates our dense sampling strategy (Sec. 4) as a critical component for achieving maximum fidelity.

Table 3. **Effect of Sample Point Density for Reconstruction.** VAE reconstruction quality consistently improves with denser input point cloud sampling, showcasing the model’s scalability.

Resolution	# of Points	PSNR $\uparrow$	SSIM $\uparrow$	LPIPS $\downarrow$
64	20,480	27.56	0.904	0.124
64	204,800	32.22	0.951	0.067
64	2,048,000	33.49	0.959	0.053
128	20,480	26.07	0.870	0.141
128	204,800	31.60	0.943	0.084
128	2,048,000	34.30	0.964	0.043
128	4,096,000	<b>34.45</b>	<b>0.965</b>	<b>0.041</b>

### 5.3. State-of-the-Art Conditional 3D Texture Generation

Having validated our core representation, we now evaluate the full LaFiTe pipeline on the end-to-end task of conditional texture generation, comparing against both image-conditioned and text-conditioned state-of-the-art baselines.

**Experimental Setup.** We curate a challenging test set designed to reflect a practical asset creation workflow. We collect approximately 800 diverse 3D meshes generated by commercial AI tools [1–3, 26, 64], using a set of 200 prompt images from various sources [17, 67, 68]. This ensures the evaluation is performed on novel, “in-the-wild” geometries rather than familiar assets from open-source training sets. For text-based methods, we use a powerful VLM (Qwen-2.5VL [5]) to generate prompts from the reference images, ensuring a fair comparison.

**Metrics and Evaluation.** We render all generated texturing results from three canonical views under both unshaded and shaded settings. For methods that do not generate PBR channels, shaded results are rendered with a default material (metallic=0, roughness=0.5). To measure the fidelity and alignment with the input condition, we compute a suite of standard generative modeling metrics: Fréchet Distance (FD) [4] and Kernel Distance (KD) [54] using feature spaces from CLIP [57] and DINO [52] to capture semantic and stylistic similarity.

**Quantitative Results.** As shown in Table 1, LaFiTe demonstrates superior performance across nearly all metrics and conditions. In the image-conditioned task, LaFiTe achieves the best or second-best scores on all metrics, significantly outperforming prior work in  $FD_{CLIP}$  and  $KD_{DINO}$  under the *shaded* setting. This confirms that our framework, which leverages a high-fidelity representation and precise 3D geometric conditioning, produces textures that are more faithful to the input prompt than any alternative method.

**Qualitative Results.** Beyond metrics, LaFiTe exhibits clear qualitative advantages, which we analyze in terms of **Integrity**, **Continuity**, and **Versatility**. As visualized in Fig. 5, our method consistently generates textures that fully

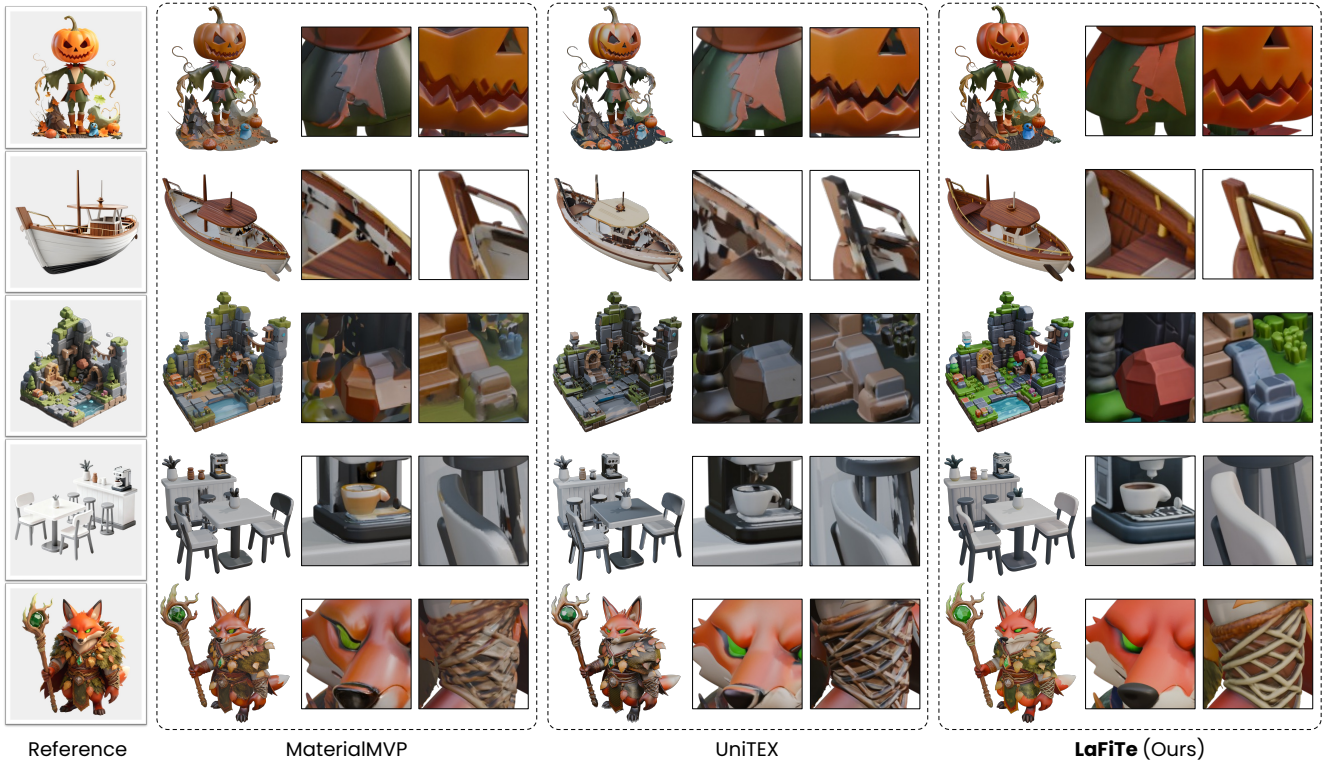


Figure 5. **Qualitative comparison of image-conditioned 3D texture generation.** Textures generated by LaFiTe are more faithfully aligned to both the reference image and the given geometry, and are free from seams or inconsistencies.

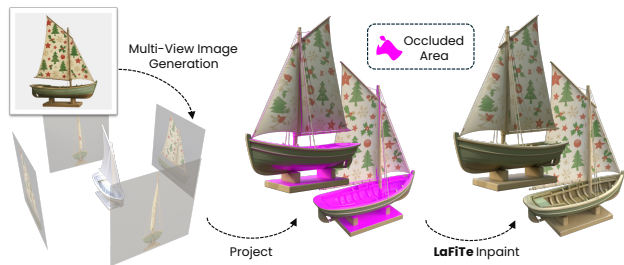


Figure 6. **Integration with multi-view projections.** LaFiTe can be used to complete occluded regions for the partial 3D texture projected from multi-view images.

cover the entire mesh (**Integrity**), are free from UV seams or projection artifacts (**Continuity**), and generalize well to a wide variety of object categories (**Versatility**). In contrast, competing methods often produce visible seams, blurred details, or incomplete textures, particularly on complex or self-occluded geometry.

#### 5.4. Downstream Applications

A key advantage of our learned latent field is its flexibility. We demonstrate its power through several applications:

- **Integration with Multi-View Pipelines:** The structured latent representation enables LaFiTe to be easily inte-



Figure 7. **Material Transfer.** LaFiTe can generate textures with PBR materials conditioned on a 2D material image.

grated with multi-view projections by inpainting the unseen area. Fig. 6 shows that our method can robustly fill occluded regions while keeping the projected areas unchanged.

- **Material Transfer:** Fig. 7 demonstrates direct material transfer, where a 2D material image is used as the image condition to synthesize seamless PBR textures on the mesh.
- **Local Refinement:** Fig. 8 shows an example of local texture refinement using our method, resulting in a much higher level of local details.

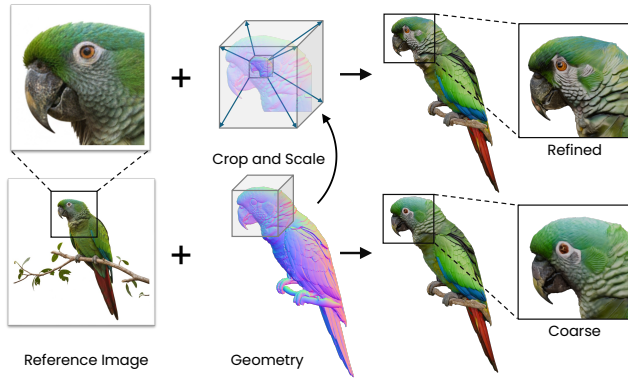


Figure 8. **Local Refinement.** LaFiTe can further enhance the generation quality by refining a local region.

## 6. Conclusion

We introduced LaFiTe, a generative framework that fundamentally advances native 3D texturing. We identified the critical bottleneck as the lack of a powerful, topology-agnostic representation and solved it by learning to generate textures as a 3D structured latent color field. Our VAE-based representation achieves state-of-the-art fidelity, and our unified design for geometric conditioning ensures seamless, high-quality generation. By solving this core representation problem, LaFiTe significantly outperforms existing methods and provides a robust foundation for future 3D generative workflows.

**Limitations and Future Work.** Lafite’s 3D-native approach lacks the priors of large-scale 2D generation models compared to multi-view-based 3D texturing methods, limiting its ability on semantic soundness and text rendering quality. Future work may explore leveraging the vast prior knowledge embedded in large-scale image and video datasets to mitigate the scarcity of high-quality textured 3D training data.

## References

- [1] Tripo AI. Tripo ai – create your first 3d model with text and image. <https://www.tripo3d.ai/>, 2025. 7
- [2] Hyper3D / Rodin AI. Rodin – free ai 3d model generator for everyone. <https://hyper3d.ai/>, 2025.
- [3] Meshy AI. Meshy ai – meet the world’s most popular and intuitive free ai 3d model generator. <https://www.meshy.ai/>, 2025. 7
- [4] Helmut Alt and Michael Godau. Computing the fréchet distance between two polygonal curves. In *International Colloquium on Automata, Languages, and Programming (ICALP)*, pages 327–338. Springer, 1995. 7
- [5] Shuai Bai, Keqin Chen, Xuejing Liu, Jialin Wang, Wenbin Ge, Sibao Song, Kai Dang, Peng Wang, Shijie Wang, Jun Tang, Humen Zhong, Yuanzhi Zhu, Mingkun Yang, Zhaohai Li, Jianqiang Wan, Pengfei Wang, Wei Ding, Zheren Fu, Yiheng Xu, Jiabo Ye, Xi Zhang, Tianbao Xie, Zesen Cheng, Hang Zhang, Zhibo Yang, Haiyang Xu, and Junyang Lin. Qwen2.5-vl technical report. *arXiv preprint arXiv:2502.13923*, 2025. 7
- [6] Raphael Bensch, Yanir Kleiman, Idan Azuri, Omri Harosh, Andrea Vedaldi, Natalia Neverova, and Oran Gafni. Meta 3d texturegen: Fast and consistent texture generation for 3d objects. *arXiv preprint arXiv:2407.02430*, 2024. 3
- [7] Michael Birsak, John Femiani, Biao Zhang, and Peter Wonka. Matclip: Light-and shape-insensitive assignment of pbr material models. In *Proceedings of the Special Interest Group on Computer Graphics and Interactive Techniques Conference Conference Papers*, pages 1–10, 2025. 3
- [8] Tianshi Cao, Karsten Kreis, Sanja Fidler, Nicholas Sharp, and Kangxue Yin. Textfusion: Synthesizing 3d textures with text-guided image diffusion models. In *Proceedings of the IEEE/CVF international conference on computer vision*, pages 4169–4181, 2023. 3
- [9] Eric R Chan, Connor Z Lin, Matthew A Chan, Koki Nagano, Boxiao Pan, Shalini De Mello, Orazio Gallo, Leonidas J Guibas, Jonathan Tremblay, Sameh Khamis, et al. Efficient geometry-aware 3d generative adversarial networks. In *Proceedings of the IEEE/CVF conference on computer vision and pattern recognition*, pages 16123–16133, 2022. 3
- [10] Dave Zhenyu Chen, Yawar Siddiqui, Hsin-Ying Lee, Sergey Tulyakov, and Matthias Nießner. Text2tex: Text-driven texture synthesis via diffusion models. In *Proceedings of the IEEE/CVF international conference on computer vision*, pages 18558–18568, 2023. 2, 3
- [11] Rui Chen, Yongwei Chen, Ningxin Jiao, and Kui Jia. Fantasia3d: Disentangling geometry and appearance for high-quality text-to-3d content creation. In *Proceedings of the IEEE/CVF international conference on computer vision*, pages 22246–22256, 2023. 3
- [12] Yiwen Chen, Tong He, Di Huang, Weicai Ye, Sijin Chen, Jiaxiang Tang, Xin Chen, Zhongang Cai, Lei Yang, Gang Yu, et al. Meshanything: Artist-created mesh generation with autoregressive transformers. *arXiv preprint arXiv:2406.10163*, 2024. 2
- [13] Zhiqin Chen and Hao Zhang. Learning implicit fields for generative shape modeling. In *Proceedings of the IEEE/CVF Conference on Computer Vision and Pattern Recognition (CVPR)*, 2019. 2
- [14] Wei Cheng, Juncheng Mu, Xianfang Zeng, Xin Chen, Anqi Pang, Chi Zhang, Zhibin Wang, Bin Fu, Gang Yu, Ziwei Liu, et al. Mypaint: Synchronized multi-view diffusion for painting anything 3d. In *Proceedings of the Computer Vision and Pattern Recognition Conference*, pages 585–594, 2025. 3, 6
- [15] Matt Deitke, Ruoshi Liu, Matthew Wallingford, Huong Ngo, Oscar Michel, Aditya Kusupati, Alan Fan, Christian Laforte, Vikram Voleti, Samir Yitzhak Gadre, et al. Objaverse-xl: A universe of 10m+ 3d objects. *Advances in Neural Information Processing Systems*, 36:35799–35813, 2023. 5, 6
- [16] Matt Deitke, Dustin Schwenk, Jordi Salvador, Luca Weihs, Oscar Michel, Eli VanderBilt, Ludwig Schmidt, Kiana Ehsani, Aniruddha Kembhavi, and Ali Farhadi. Objaverse: A universe of annotated 3d objects. In *Proceedings of*

- the *IEEE/CVF conference on computer vision and pattern recognition*, pages 13142–13153, 2023. 5, 6
- [17] Dylan Ebert. 3d arena: An open platform for generative 3d evaluation. *arXiv preprint arXiv:2506.18787*, 2025. 7
- [18] Ye Fang, Zeyi Sun, Tong Wu, Jiaqi Wang, Ziwei Liu, Gordon Wetzstein, and Dahua Lin. Make-it-real: Unleashing large multimodal model’s ability for painting 3d objects with realistic materials. *CoRR*, 2024. 3
- [19] Chenjian Gao, Boyan Jiang, Xinghui Li, Yingpeng Zhang, and Qian Yu. Genesisstex: adapting image denoising diffusion to texture space. In *Proceedings of the IEEE/CVF conference on computer vision and pattern recognition*, pages 4620–4629, 2024. 3
- [20] Cindy M. Goral, Kenneth E. Torrance, Donald P. Greenberg, and Bennett Battaile. Modeling the interaction of light between diffuse surfaces. In *Proceedings of the 11th Annual Conference on Computer Graphics and Interactive Techniques (SIGGRAPH '84)*, pages 213–222, New York, NY, USA, 1984. ACM. 5
- [21] Benoit Guillard, Federico Stella, and Pascal Fua. Meshudf: Fast and differentiable meshing of unsigned distance field networks. In *European Conference on Computer Vision*, 2022. 2
- [22] Yanhui Guo, Xinxin Zuo, Peng Dai, Juwei Lu, Xiaolin Wu, Youliang Yan, Songcen Xu, Xiaofei Wu, et al. Decorate3d: text-driven high-quality texture generation for mesh decoration in the wild. *Advances in Neural Information Processing Systems*, 36:36664–36676, 2023. 3
- [23] Yuan-Chen Guo, Ying-Tian Liu, Ruizhi Shao, Christian Laforte, Vikram Voleti, Guan Luo, Chia-Hao Chen, Zi-Xin Zou, Chen Wang, Yan-Pei Cao, et al. threestudio: A unified framework for 3d content generation, 2023. 2
- [24] Xianglong He, Zi-Xin Zou, Chia-Hao Chen, Yuan-Chen Guo, Ding Liang, Chun Yuan, Wanli Ouyang, Yan-Pei Cao, and Yangguang Li. Sparseflex: High-resolution and arbitrary-topology 3d shape modeling. *arXiv preprint arXiv:2503.21732*, 2025. 3, 4
- [25] Zebin He, Mingxin Yang, Shuhui Yang, Yixuan Tang, Tao Wang, Kaihao Zhang, Guanying Chen, Yuhong Liu, Jie Jiang, Chunchao Guo, et al. Materialmvp: Illumination-invariant material generation via multi-view pbr diffusion. *arXiv preprint arXiv:2503.10289*, 2025. 2, 3, 5, 6
- [26] HiTem3D. Hitem3d: Next-gen ai 3d model generator. <https://hitem3d.ai/>, 2025. 7
- [27] Yijia Hong, Yuan-Chen Guo, Ran Yi, Yulong Chen, Yan-Pei Cao, and Lizhuang Ma. Supermat: Physically consistent pbr material estimation at interactive rates. *arXiv preprint arXiv:2411.17515*, 2024. 3
- [28] Yicong Hong, Kai Zhang, Jiuxiang Gu, Sai Bi, Yang Zhou, Difan Liu, Feng Liu, Kalyan Sunkavalli, Trung Bui, and Hao Tan. LRM: Large reconstruction model for single image to 3d. In *The Twelfth International Conference on Learning Representations*, 2024. 3
- [29] Yijia Hong, Yuan-Chen Guo, Ran Yi, Yulong Chen, Yan-Pei Cao, and Lizhuang Ma. Supermat: Physically consistent pbr material estimation at interactive rates. In *Proceedings of the IEEE/CVF International Conference on Computer Vision*, pages 25083–25093, 2025. 3
- [30] Xin Huang, Tengfei Wang, Ziwei Liu, and Qing Wang. Material anything: Generating materials for any 3d object via diffusion. In *Proceedings of the Computer Vision and Pattern Recognition Conference*, pages 26556–26565, 2025. 3, 6
- [31] Zehuan Huang, Yuan-Chen Guo, Haoran Wang, Ran Yi, Lizhuang Ma, Yan-Pei Cao, and Lu Sheng. Mv-adapter: Multi-view consistent image generation made easy. In *Proceedings of the IEEE/CVF International Conference on Computer Vision*, pages 16377–16387, 2025. 3
- [32] Dong Huo, Zixin Guo, Xinxin Zuo, Zhihao Shi, Juwei Lu, Peng Dai, Songcen Xu, Li Cheng, and Yee-Hong Yang. Texgen: Text-guided 3d texture generation with multi-view sampling and resampling. In *European Conference on Computer Vision*, pages 352–368. Springer, 2024. 3
- [33] Bernhard Kerbl, Georgios Kopanas, Thomas Leimkühler, and George Drettakis. 3d gaussian splatting for real-time radiance field rendering. *ACM Trans. Graph.*, 42(4):139–1, 2023. 2
- [34] Peter Kocsis, Lukas Höllein, and Matthias Nießner. Intrinsic: High-quality pbr generation using image priors. *arXiv preprint arXiv:2504.01008*, 2025. 3
- [35] Black Forest Labs, Stephen Batifol, Andreas Blattmann, Frederic Boesel, Saksham Consul, Cyril Diagne, Tim Dockhorn, Jack English, Zion English, Patrick Esser, Sumith Kulal, Kyle Lacey, Yam Levi, Cheng Li, Dominik Lorenz, Jonas Müller, Dustin Podell, Robin Rombach, Harry Saini, Axel Sauer, and Luke Smith. Flux.1 kontext: Flow matching for in-context image generation and editing in latent space, 2025. 5
- [36] Jiahao Li, Hao Tan, Kai Zhang, Zexiang Xu, Fujun Luan, Yinghao Xu, Yicong Hong, Kalyan Sunkavalli, Greg Shakhnarovich, and Sai Bi. Instant3d: Fast text-to-3d with sparse-view generation and large reconstruction model. In *The Twelfth International Conference on Learning Representations*, 2024. 3
- [37] Yangguang Li, Zi-Xin Zou, Zexiang Liu, Dehu Wang, Yuan Liang, Zhipeng Yu, Xingchao Liu, Yuan-Chen Guo, Ding Liang, Wanli Ouyang, et al. Triposg: High-fidelity 3d shape synthesis using large-scale rectified flow models. *arXiv preprint arXiv:2502.06608*, 2025. 3
- [38] Zhihao Li, Yufei Wang, Heliang Zheng, Yihao Luo, and Bihan Wen. Sparc3d: Sparse representation and construction for high-resolution 3d shapes modeling. *arXiv preprint arXiv:2505.14521*, 2025. 3
- [39] Yixun Liang, Xin Yang, Jiantao Lin, Haodong Li, Xiaogang Xu, and Yingcong Chen. Luciddreamer: Towards high-fidelity text-to-3d generation via interval score matching. In *Proceedings of the IEEE/CVF conference on computer vision and pattern recognition*, pages 6517–6526, 2024. 2
- [40] Yixun Liang, Kunming Luo, Xiao Chen, Rui Chen, Hongyu Yan, Weiyu Li, Jiarui Liu, and Ping Tan. Unitex: Universal high fidelity generative texturing for 3d shapes. *arXiv preprint arXiv:2505.23253*, 2025. 2, 3, 6
- [41] Jialun Liu, Chenming Wu, Xinqi Liu, Xing Liu, Jinbo Wu, Haotian Peng, Chen Zhao, Haocheng Feng, Jingtuo Liu, and Errui Ding. Texoct: Generating textures of 3d models with

- octree-based diffusion. In *Proceedings of the IEEE/CVF Conference on Computer Vision and Pattern Recognition*, pages 4284–4293, 2024. 3
- [42] Xingchao Liu, Chengyue Gong, and Qiang Liu. Flow straight and fast: Learning to generate and transfer data with rectified flow, 2022. 5
- [43] Yuxin Liu, Minshan Xie, Hanyuan Liu, and Tien-Tsin Wong. Text-guided texturing by synchronized multi-view diffusion. In *SIGGRAPH Asia 2024 Conference Papers*, pages 1–11, 2024. 2, 3, 5, 6
- [44] Ilya Loshchilov and Frank Hutter. Decoupled weight decay regularization. In *International Conference on Learning Representations (ICLR)*, 2019. 6
- [45] Jiawei Lu, Yingpeng Zhang, Zengjun Zhao, He Wang, Kun Zhou, and Tianjia Shao. Genesis2: Stable, consistent and high-quality text-to-texture generation. In *Proceedings of the AAAI Conference on Artificial Intelligence*, pages 5820–5828, 2025. 3
- [46] Andreas Lugmayr, Martin Danelljan, Andres Romero, Fisher Yu, Radu Timofte, and Luc Van Gool. Repaint: Inpainting using denoising diffusion probabilistic models. In *Proceedings of the IEEE/CVF conference on computer vision and pattern recognition*, pages 11461–11471, 2022. 5
- [47] Thomas Müller, Alex Evans, Christoph Schied, and Alexander Keller. Instant neural graphics primitives with a multiresolution hash encoding. *ACM Trans. Graph.*, 41(4):102:1–102:15, 2022. 3
- [48] Jacob Munkberg, Zian Wang, Ruofan Liang, Tianchang Shen, and Jon Hasselgren. Videomat: Extracting pbr materials from video diffusion models. In *Computer Graphics Forum*, page e70180. Wiley Online Library, 2025. 3
- [49] Charlie Nash, Yaroslav Ganin, SM Ali Eslami, and Peter Battaglia. Polygen: An autoregressive generative model of 3d meshes. In *International conference on machine learning*, pages 7220–7229. PMLR, 2020. 2
- [50] Tomoyuki Nishita and Eihachiro Nakamae. Continuous tone representation of three-dimensional objects taking account of shadows and interreflection. In *Proceedings of the 12th Annual Conference on Computer Graphics and Interactive Techniques (SIGGRAPH '85)*, pages 23–30, New York, NY, USA, 1985. ACM. 5
- [51] Michael Oechsle, Lars Mescheder, Michael Niemeyer, Thilo Strauss, and Andreas Geiger. Texture fields: Learning texture representations in function space. In *Proceedings of the IEEE/CVF international conference on computer vision*, pages 4531–4540, 2019. 2, 3
- [52] Maxime Oquab, Timothée Darcet, Theo Moutakanni, Huy V. Vo, Marc Szafraniec, Vasil Khalidov, Pierre Fernandez, Daniel Haziza, Francisco Massa, Alaaeldin El-Nouby, Russell Howes, Po-Yao Huang, Hu Xu, Vasu Sharma, Shang-Wen Li, Wojciech Galuba, Mike Rabbat, Mido Assran, Nicolas Ballas, Gabriel Synnaeve, Ishan Misra, Herve Jegou, Julien Mairal, Patrick Labatut, Armand Joulin, and Piotr Bojanowski. Dinov2: Learning robust visual features without supervision, 2023. 3, 6, 7
- [53] Jeong Joon Park, Peter Florence, Julian Straub, Richard Newcombe, and Steven Lovegrove. Deepsdf: Learning continuous signed distance functions for shape representation. In *Proceedings of the IEEE/CVF Conference on Computer Vision and Pattern Recognition (CVPR)*, pages 165–174, 2019. 2
- [54] Jeff M. Phillips and Suresh Venkatasubramanian. A geometric approach to comparing datasets via kernel distance. In *Proceedings of the 27th Annual Symposium on Computational Geometry (SoCG)*, pages 317–326. ACM, 2011. 7
- [55] Ben Poole, Ajay Jain, Jonathan T. Barron, and Ben Mildenhall. Dreamfusion: Text-to-3d using 2d diffusion. In *The Eleventh International Conference on Learning Representations*, 2023. 2
- [56] Charles R Qi, Hao Su, Kaichun Mo, and Leonidas J Guibas. Pointnet: Deep learning on point sets for 3d classification and segmentation. In *Proceedings of the IEEE conference on computer vision and pattern recognition*, pages 652–660, 2017. 3
- [57] Alec Radford, Jong Wook Kim, Chris Hallacy, Aditya Ramesh, Gabriel Goh, Sandhini Agarwal, Girish Sastry, Amanda Askell, Pamela Mishkin, Jack Clark, Gretchen Krueger, and Ilya Sutskever. Learning transferable visual models from natural language supervision. In *Proceedings of the 38th International Conference on Machine Learning (ICML)*, pages 8748–8763. PMLR, 2021. 7
- [58] Elad Richardson, Gal Metzer, Yuval Alaluf, Raja Giryes, and Daniel Cohen-Or. Texture: Text-guided texturing of 3d shapes. In *ACM SIGGRAPH 2023 conference proceedings*, pages 1–11, 2023. 3
- [59] J Ryan Shue, Eric Ryan Chan, Ryan Po, Zachary Ankner, Jiajun Wu, and Gordon Wetzstein. 3d neural field generation using triplane diffusion. In *Proceedings of the IEEE/CVF Conference on Computer Vision and Pattern Recognition*, pages 20875–20886, 2023. 3
- [60] Yawar Siddiqui, Justus Thies, Fangchang Ma, Qi Shan, Matthias Nießner, and Angela Dai. Texturify: Generating textures on 3d shape surfaces. In *European Conference on Computer Vision*, pages 72–88. Springer, 2022. 3
- [61] Yawar Siddiqui, Antonio Alliegro, Alexey Artemov, Tatiana Tommasi, Daniele Sirigatti, Vladislav Rosov, Angela Dai, and Matthias Nießner. Meshgpt: Generating triangle meshes with decoder-only transformers. In *Proceedings of the IEEE/CVF conference on computer vision and pattern recognition*, pages 19615–19625, 2024. 2
- [62] Yawar Siddiqui, Tom Monnier, Filippos Kokkinos, Mahendra Kariya, Yanir Kleiman, Emilien Garreau, Oran Gafni, Natalia Neverova, Andrea Vedaldi, Roman Shapovalov, et al. Meta 3d assetgen: Text-to-mesh generation with high-quality geometry, texture, and pbr materials. *Advances in Neural Information Processing Systems*, 37:9532–9564, 2024. 3
- [63] Oriane Siméoni, Huy V. Vo, Maximilian Seitzer, Federico Baldassarre, Maxime Oquab, Cijo Jose, Vasil Khalidov, Marc Szafraniec, Seungeun Yi, Michaël Ramamonjisoa, Francisco Massa, Daniel Haziza, Luca Wehrstedt, Jianyuan Wang, Timothée Darcet, Théo Moutakanni, Leonel Sentana, Claire Roberts, Andrea Vedaldi, Jamie Tolan, John Brandt, Camille Couprie, Julien Mairal, Hervé Jégou, Patrick Labatut, and Piotr Bojanowski. DINOv3, 2025. 3

- [64] Tencent Hunyuan3D Team. Tencent hunyuan3d. <https://3d.hunyuan.tencent.com/>, 2025. 3, 7
- [65] Haochen Wang, Xiaodan Du, Jiahao Li, Raymond A Yeh, and Greg Shakhnarovich. Score jacobian chaining: Lifting pretrained 2d diffusion models for 3d generation. In *Proceedings of the IEEE/CVF conference on computer vision and pattern recognition*, pages 12619–12629, 2023. 2
- [66] Zhengyi Wang, Cheng Lu, Yikai Wang, Fan Bao, Chongxuan Li, Hang Su, and Jun Zhu. Prolificdreamer: High-fidelity and diverse text-to-3d generation with variational score distillation. *Advances in neural information processing systems*, 36: 8406–8441, 2023. 2
- [67] Shuang Wu, Youtian Lin, Feihu Zhang, Yifei Zeng, Yikang Yang, Yajie Bao, Jiachen Qian, Siyu Zhu, Xun Cao, Philip Torr, et al. Direct3d-s2: Gigascale 3d generation made easy with spatial sparse attention. *arXiv preprint arXiv:2505.17412*, 2025. 3, 7
- [68] Jianfeng Xiang, Zelong Lv, Sicheng Xu, Yu Deng, Ruicheng Wang, Bowen Zhang, Dong Chen, Xin Tong, and Jiaolong Yang. Structured 3d latents for scalable and versatile 3d generation. In *Proceedings of the Computer Vision and Pattern Recognition Conference*, pages 21469–21480, 2025. 2, 3, 4, 6, 7
- [69] Zhiyu Xie, Yuqing Zhang, Xiangjun Tang, Yiqian Wu, Dehan Chen, Gongsheng Li, and Xiaogang Jin. Styletex: Style image-guided texture generation for 3d models. *ACM Transactions on Graphics (TOG)*, 43(6):1–14, 2024. 3
- [70] Bojun Xiong, Jialun Liu, Jiakui Hu, Chenming Wu, Jinbo Wu, Xing Liu, Chen Zhao, Errui Ding, and Zhouhui Lian. Texgaussian: Generating high-quality pbr material via octree-based 3d gaussian splatting. In *Proceedings of the Computer Vision and Pattern Recognition Conference*, pages 551–561, 2025. 3
- [71] Dongyu Yan, Leyi Wu, Jiantao Lin, Luozhou Wang, Tianshuo Xu, Zhifei Chen, Zhen Yang, Lie Xu, Shunsi Zhang, and Yingcong Chen. Flexpainter: Flexible and multi-view consistent texture generation. *arXiv preprint arXiv:2506.02620*, 2025. 3
- [72] Yu-Ying Yeh, Jia-Bin Huang, Changil Kim, Lei Xiao, Thu Nguyen-Phuoc, Numair Khan, Cheng Zhang, Manmohan Chandraker, Carl S Marshall, Zhao Dong, et al. Texture-dreamer: Image-guided texture synthesis through geometry-aware diffusion. In *Proceedings of the IEEE/CVF Conference on Computer Vision and Pattern Recognition*, pages 4304–4314, 2024. 3
- [73] Xin Yu, Peng Dai, Wenbo Li, Lan Ma, Zhengzhe Liu, and Xiaojuan Qi. Texture generation on 3d meshes with point-uv diffusion. In *Proceedings of the IEEE/CVF International Conference on Computer Vision*, pages 4206–4216, 2023. 3
- [74] Xin Yu, Yuan-Chen Guo, Yangguang Li, Ding Liang, Song-Hai Zhang, and Xiaojuan Qi. Text-to-3d with classifier score distillation. *arXiv preprint arXiv:2310.19415*, 2023. 2
- [75] Xin Yu, Ze Yuan, Yuan-Chen Guo, Ying-Tian Liu, Jianhui Liu, Yangguang Li, Yan-Pei Cao, Ding Liang, and Xiaojuan Qi. Texgen: a generative diffusion model for mesh textures. *ACM Transactions on Graphics (TOG)*, 43(6):1–14, 2024. 2, 3, 6
- [76] Ze Yuan, Xin Yu, Yangtian Sun, Yuan-Chen Guo, Yan-Pei Cao, Ding Liang, and Xiaojuan Qi. Seqtex: Generate mesh textures in video sequence. *arXiv preprint arXiv:2507.04285*, 2025. 3, 6
- [77] Xianfang Zeng, Xin Chen, Zhongqi Qi, Wen Liu, Zibo Zhao, Zhibin Wang, Bin Fu, Yong Liu, and Gang Yu. Paint3d: Paint anything 3d with lighting-less texture diffusion models. In *Proceedings of the IEEE/CVF conference on computer vision and pattern recognition*, pages 4252–4262, 2024. 6
- [78] Zheng Zeng, Valentin Deschaintre, Iliyan Georgiev, Yannick Hold-Geoffroy, Yiwei Hu, Fujun Luan, Ling-Qi Yan, and Miloš Hašan. Rgb $\leftrightarrow$ x: Image decomposition and synthesis using material- and lighting-aware diffusion models. In *ACM SIGGRAPH 2024 Conference Papers*, New York, NY, USA, 2024. Association for Computing Machinery. 3
- [79] Biao Zhang, Jiapeng Tang, Matthias Niessner, and Peter Wonka. 3dshape2vecset: A 3d shape representation for neural fields and generative diffusion models. *ACM Transactions On Graphics (TOG)*, 42(4):1–16, 2023. 2, 3
- [80] Kai Zhang, Sai Bi, Hao Tan, Yuanbo Xiangli, Nanxuan Zhao, Kalyan Sunkavalli, and Zexiang Xu. Gs-lrm: Large reconstruction model for 3d gaussian splatting. In *European Conference on Computer Vision*, pages 1–19. Springer, 2024. 3
- [81] Longwen Zhang, Ziyu Wang, Qixuan Zhang, Qiwei Qiu, Anqi Pang, Haoran Jiang, Wei Yang, Lan Xu, and Jingyi Yu. Clay: A controllable large-scale generative model for creating high-quality 3d assets. *ACM Transactions on Graphics (TOG)*, 43(4):1–20, 2024. 3
- [82] Yuqing Zhang, Yuan Liu, Zhiyu Xie, Lei Yang, Zhongyuan Liu, Mengzhou Yang, Runze Zhang, Qilong Kou, Cheng Lin, Wenping Wang, et al. Dreammat: High-quality pbr material generation with geometry-and light-aware diffusion models. *ACM Transactions on Graphics (TOG)*, 43(4):1–18, 2024. 3
- [83] Yibo Zhang, Li Zhang, Rui Ma, and Nan Cao. Texverse: A universe of 3d objects with high-resolution textures. *arXiv preprint arXiv:2508.10868*, 2025. 6
- [84] Shenhao Zhu, Lingteng Qiu, Xiaodong Gu, Zhengyi Zhao, Chao Xu, Yuxiao He, Zhe Li, Xiaoguang Han, Yao Yao, Xun Cao, et al. Mcmat: Multiview-consistent and physically accurate pbr material generation. *arXiv preprint arXiv:2412.14148*, 2024. 3
- [85] Zi-Xin Zou, Zhipeng Yu, Yuan-Chen Guo, Yangguang Li, Ding Liang, Yan-Pei Cao, and Song-Hai Zhang. Triplane meets gaussian splatting: Fast and generalizable single-view 3d reconstruction with transformers. In *Proceedings of the IEEE/CVF conference on computer vision and pattern recognition*, pages 10324–10335, 2024. 3